

Electronic Isomerism: Symmetry Breaking and Electronic Phase Diagrams for Diatomic Molecules at the Large-Dimension Limit

Qicun Shi,^[b] Sabre Kais,^[a, b] Françoise Remacle,^[a, c] and Raphael D. Levine^{*[a]}

We present symmetry-breaking and electronic-structure phase diagrams for two-center molecules with one and two electrons in the limit of a space of large dimensions. For one electron, the phase diagram in the internuclear distance–nuclear charge ($R-Z$) plane has two different stable phases. One corresponds to the electron equidistant from the two nuclei; the other where the electron is localized on one of the nuclei. The phase diagram for two electrons with two equally charged centers shows three different stable phases corresponding to different electronic-structure configurations. This phase diagram is characterized by a bicritical point. When the charges are unequal, the phase diagram shows only two stable phases, covalent and ionic. This phase diagram is charac-

terized by a tricritical point, where the first-order transition line meets with the second-order transition line. The role of the inter-electron Coulombic repulsion in giving rise to different electronic structures and the distinction between a continuous deformation of one structure into another versus a discontinuous, so-called first-order, transition, where two isomers can coexist, are emphasized. The connection to the spectroscopic notion of intersecting potential energy curves is discussed.

KEYWORDS:

curve crossing · dimensional scaling · Jahn–Teller distortion · phase transitions

Introduction

Polyatomic molecules in their ground electronic state can have more than one stable configuration (isomer). An example of two isomers are cyclohexadiene and hexatriene, where the ring is open or closed, Figure 1. Typically, the different isomers are obtained by varying the interatomic distances (directly or indirectly; see ref. [1] for the details of an indirect route for the isomerization as shown in Figure 1). In the Born–Oppenheimer

approximation^[2, 3] these distances are treated as parameters of the electronic Hamiltonian. Changing the parameters changes the Hamiltonian, and more than one electronic conformation is therefore potentially possible. We have recently discussed the options for more subtle tunings of the electronic Hamiltonian by using quantum dots and discussed the rather rich phase diagram of isomers that is thereby made possible.^[4]

Our work on quantum dots suggests that the different isomers correspond to different distributions of electronic charge over the nuclear framework. In particular, the quantum phase transition that we believe has been seen experimentally^[5] corresponds to a transition from a localized to a delocalized distribution of charge. We have pointed out that such a transition can be discerned even in a diatomic molecule. But, in an ordinary diatomic molecule, this transition is not sharp.

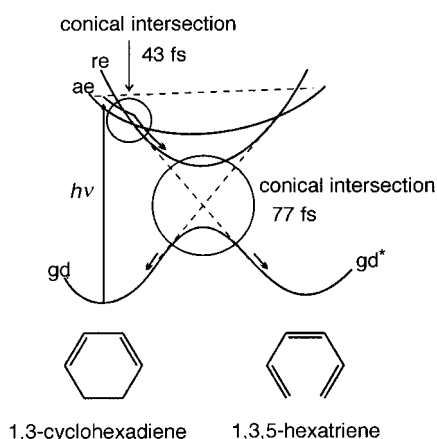


Figure 1. An experimentally realizable^[1] scheme for electrocyclic ring opening in cyclohexadiene.^[27] The indirect route, through two conical intersections, allows one minimum on the ground potential energy surface to be reached from another. gd and gd^* refer to the ground electronic states of the two isomers, ae and re refer to two excited states.

[a] Prof. R. D. Levine, Prof. S. Kais, Dr. F. Remacle
The Fritz Haber Research Center for Molecular Dynamics
The Hebrew University, Jerusalem 91904 (Israel)
Fax: 972-2-6513742
E-mail: rafi@fh.huji.ac.il

[b] Q. Shi, Prof. S. Kais
Department of Chemistry
Purdue University
West Lafayette, IN 47907 (USA)

[c] Dr. F. Remacle
Département de Chimie, B6b
Université Liège
4000 Liège (Belgium)

Technically, a measure of the uneven charge distribution is the ratio of the “charge orders”^[12] of the two atoms. In a two-state problem, it is given as $C_2/C_1 = \tan(\theta)$, where the angle θ is defined in terms of the energy difference ΔE between the two centers and their coupling V by $\Delta E/V = \cot(2\theta)$, as shown in Figure 2. The rapid variation is quite evident, but unless one has the benefit of familiarity with the more general case, it would not be persuasive to call it a “transition”. So, we searched for an alternative way to discuss the possible quantum phase space, with special reference to the effect of variations in the two-site energies. (By “site energy” we mean the energy of the electron when it is on one center and the other center is considered far away.)

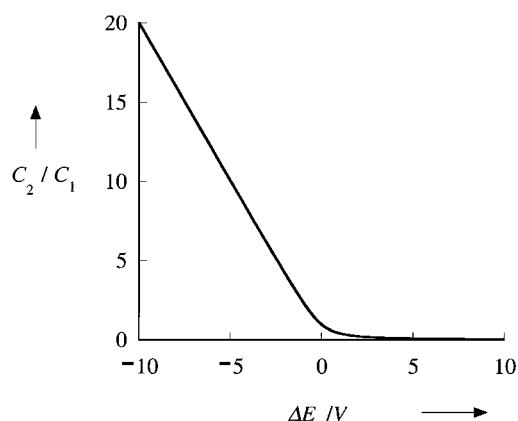


Figure 2. The division of the total electronic charge (one unit) between two centers which differ in their site energies by ΔE as a function of ΔE (scaled by the coupling V between the two centers), $\Delta E/V = \cot(2\theta)$ with $C_2/C_1 = \tan(\theta)$. The Figure is computed for the ground state. For the excited state, the picture is reversed and can be visualized by reflecting this Figure along the $\Delta E = 0$ vertical and then along the $\tan(\theta) = 0$ horizontal axes. In the following, we will vary the site energies by varying the nuclear charge.

Dimensional scaling^[6] does seem to offer the required tool. In this approach, the dimension D of the space available for the motion of the electron is increased above the physical value, $D = 3$. As has been often discussed, in the large-dimension limit, the method recovers the Lewis picture of the chemical bond with electrons localized in the bonding region.^[7] Moreover, the first correction of order $1/D$ is equivalent to Langmuir’s picture of electrons harmonically oscillating about their equilibrium position.

We supplement the large- D analysis by the technical notion of a quantum phase transition.^[8] For the moment, we carry the analysis for the electronic ground state (namely at the limit of temperature approaching zero) so that the problem reduces to the determination of the singularities of the energy (rather than of the free energy). The combination of a large- D limit and an analysis of the singularities in the phase plane has been previously applied to homonuclear diatomic molecules,^[9] and we also refer to ref. [10] for a more general review.

One might question if the large- D limit is sufficient for a discussion of electronic isomerism because one expects

that rearrangement of the charge distribution is driven by a competition between the kinetic and potential energy terms with the kinetic energy favoring delocalization. As is known, and as will be shown below, the simplicity of the large- D limit is afforded because the electron behaves as if it has a mass which scales as D and therefore only the electrostatic terms of the Hamiltonian survive in the large- D limit. This is almost but not quite correct. It will be shown that the rotational part of the kinetic energy does remain in the large- D limit and that it suffices to recover the expected transition from the localized to delocalized states.

In this Article, we only point out the connection between the quantum phase transitions that we identify and the quantum-chemical notion of curve crossing.^[11, 12] Specifically, we comment that what is known as a “second-order” phase transition, when present for two electronic configurations, has a molecular analog in the Renner–Teller intersection.^[11–14] This is a continuous transition where the energies diverge quadratically from their intersection. The “first-order” phase transition has as its molecular analog the Jahn–Teller intersection, also known nowadays as a conical intersection, where the energies diverge linearly^[15] from the point of the intersection. We draw attention to these analogies early because we discuss phase transitions in a diatomic molecule. The very familiar noncrossing rule^[16–18] seems, at first sight, to disallow such intersections. Here, we only point out that we are not in conflict with the usual proofs of the rule because these specifically depend on only one parameter being varied. As soon as more than one parameter is considered, intersections are possible.^[15] An Appendix provides the technical backing of this point for our problem. We are aware that there is a rich literature dealing with the validity of the noncrossing rule in diatomic molecules (see, for example, refs. [19, 20]). We only note that the usual proofs do not apply to our case because we allow more than one parameter to vary. It is in this context that the notion of “designer atoms”,^[4] where one can tune the parameters of the Hamiltonian, becomes particularly relevant.

There were three parameters in the study^[4, 21] of electronic isomerism for assemblies of quantum dots. We discuss here the correspondence between these and the parameters of the Hamiltonian when it is written in terms of Coulombic forces between electrons and nuclei. We do so for the special case of a two-center, one or two electron, molecule that will be analyzed in detail later. The first parameter governs the magnitude of the ionization potential of a single center. We here take the charge Z on the nucleus as the corresponding parameter. Since each isolated center has one electron, the Bohr formula tells us that the ionization potential scales as Z . The second parameter is the magnitude of the Coulombic repulsion between two electrons. This repulsion will here be treated exactly. The third parameter is the electronic coupling between the two centers. This parameter was varied by varying the distance R between the centers. Herein, we do the same. The electrostatic attraction of an electron to the “other” center is written explicitly and so it is a function of the separation between the two centers.

The Large- D Hamiltonian for Two Coulomb Centers with Charges Z_a and Z_b

We treat the case of one and two electrons in the field of two Coulomb centers of charges Z_a and Z_b at the large-dimensional limit.^[6] The Born–Oppenheimer approximation is used to separate the electronic and nuclear motion, so that the electronic energy $E_D(R)$ becomes parametrically dependent upon the internuclear distance R . The Hamiltonian is specified using D -dimensional cylindrical coordinates (ρ, z) , so that the nuclei a and b are located on the z -axis at $-R/2$ and $R/2$ with charges Z_a and Z_b , respectively. Electrons 1 and 2 are located at (ρ_1, z_1) and (ρ_2, z_2) , with a dihedral angle ϕ specifying their relative azimuthal orientation about the molecular axis. The D -dimensional electronic Schrödinger equation in atomic units is given by Equation (1),^[9] where \mathcal{L}_{D-2}^2 is the D -dimensional generalized orbital angular-momentum operator and $V = V(\rho_1, \rho_2, z_1, z_2, \phi, Z_a, Z_b)$ is the potential energy of the electron–nucleus and electron–electron interactions.

$$\left[-\frac{1}{2} \sum_{i=1}^2 \left(\frac{1}{\rho_i^{D-2}} \frac{\partial}{\partial \rho_i} \rho_i^{D-2} \frac{\partial}{\partial \rho_i} + \frac{\partial^2}{\partial z_i^2} \right) + \left(\frac{1}{\rho_1^2} + \frac{1}{\rho_2^2} \right) \mathcal{L}_{D-2}^2 + V \right] \Psi = E_D(R) \Psi \quad (1)$$

An effective Hamiltonian at the large- D limit can be obtained by analogy to the introduction of a radial Hamiltonian in the ordinary, $D=3$, case. It is convenient to scale all coordinates by a factor with quadratic dependence on dimension. The scaling factor is chosen to give finite energies in the limit $D \rightarrow \infty$, while reducing to unity at $D=3$.^[6] We obtain, in units of $1/\kappa^2$ ($\kappa = (D-1)/2$) Hartree for energy and κ^2 Bohr radii for distances, the following effective large- D two electron Hamiltonian, Equation (2).

$$\mathcal{H}_\infty = \mathcal{H}_1 + \mathcal{H}_2 + \frac{1}{r_{12}} \quad (2)$$

Here, \mathcal{H}_i ($i=1, 2$) is the one-electron molecular Hamiltonian, Equation (3), and r_{12} is given by Equation (4).

$$\mathcal{H}_i = \frac{1}{2\rho_i^2} - \frac{Z_a}{\sqrt{\rho_i^2 + \left(z_i + \frac{R}{2}\right)^2}} - \frac{Z_b}{\sqrt{\rho_i^2 + \left(z_i - \frac{R}{2}\right)^2}} \quad (3)$$

$$r_{12} = \sqrt{\rho_1^2 + \rho_2^2 + (z_1 - z_2)^2 - 2\rho_1\rho_2\cos(\phi)} \quad (4)$$

The following points concerning the form of the effective Hamiltonian in the $D \rightarrow \infty$ limit are worthy of special note. First, for the case of only one electron. The full Hamiltonian is then given by Equation (3). This effective one-electron Hamiltonian has only the centrifugal energy term as the remnant of the kinetic energy. Otherwise, the only other term in the Hamiltonian is the Coulomb attraction to the two centers. Therefore, evaluating the ground-state electronic energy for $D \rightarrow \infty$ reduces to determining the minimum of a function. Already here, we note that in Equation (3) the kinetic and potential energy terms act in opposite directions: Lowering the kinetic energy favors delocalizing the electron while the potential

energy terms favor the electron being near to one of the two centers. For two electrons, the Hamiltonian is the sum of two one-electron terms plus the Coulomb repulsion between the two electrons. That the interelectron repulsion is retained at its full value is important to us because, as we already emphasized,^[4] this repulsion adds many new features to the phase diagram. We shall indeed verify this expectation below.

In the Hartree–Fock approximation, we set the dihedral angle ϕ at 90° .^[22] This is done because the Hartree–Fock wavefunction, constructed as a product of one-electron orbitals, lacks any explicit dependence on the angle ϕ . Hence, this angle enters only in the Jacobian volume element, and so, in the large- D limit, the angle is fixed at 90° .^[6] In reading those figures below which show the configuration for two-electron systems, one should keep in mind that the electrons are symmetrically located in two perpendicular planes.

Generally, the Hamiltonian is conserved under rotation \hat{P}_{rot} around the \hat{z} -axis and under reflection \hat{P}_{ref} . At $Z_a = Z_b$ there is an additional symmetry of inversion \hat{P}_{inv} about the origin $z=0$. For the eigenfunction of the Hamiltonian we also require the exchange of coordinates between the two electrons. In the case of one-electron molecules, the operation of exchanging two charges is equivalent to that of combining with \hat{P}_{inv} and \hat{P}_{rot} or \hat{P}_{ref} .

For finding the minimum-energy structure and exploring the symmetry breaking of the different electronic configurations, it is convenient to introduce spherical coordinates.^[23] The transformation from cylindrical coordinates (ρ_i, z_i) to spherical coordinates (λ_i, μ_i) is simply given by Equations (5–8).

$$\lambda_i = r_{ai} + r_{bi} \quad (5)$$

$$\mu_i = r_{ai} - r_{bi} \quad (6)$$

where

$$r_{ai}^2 = r_i^2 + \left(z_i + \frac{R}{2}\right)^2 \quad (7)$$

$$r_{bi}^2 = r_i^2 + \left(z_i - \frac{R}{2}\right)^2 \quad (8)$$

We will specify the possible electronic isomers by the coordinates ρ and z of the electrons.

For each specific symmetry, there exists a lowest-energy electronic configuration of the Hamiltonian for a given Z_a, Z_b , and R . The scaling transformation to the above Equations shows that the scaled energy depends on the ratio of the charges $q = Z_a/Z_b$. We calculate the energy by fixing q and varying both Z_a and R . The lowest energy is the one which is the global minimum with respect to the four variables $\lambda_1, \lambda_2, \mu_1$, and μ_2 in the Hartree–Fock approximation, where $\cos\phi=0$. Hence any point in the (R, Z_a) plane corresponds to a bound state and the whole plane represents the whole bound space which may be composed of specific regions.

To find the global energy minimum, we used the boundary conditions of the spheroidal coordinates, $R \leq \lambda_i < \infty$ and $-R \leq \mu_i \leq R$. We choose the initial values of λ_i and μ_i for a lowest-

energy configuration inside a rectangular mesh $-R/g \leq \mu_i \leq R/g$ and $gR \leq \lambda_i \leq gR + R_0$, with $g = 1.001$ and $R_0 = 5$ (a.u.). The interval of one side of the mesh is $2R/fg$ at $f = 20$. If there is no negative energy value found then we doubled R_0 and f . This defined mesh assists us in getting a good initial guess for the optimized variables before using Powell's quadratically convergent method.^[24] The intervals of R and Z_a are fixed at 0.001 (a.u.). The criterion for $\rho_1 = \rho_2$ and $z_1 = z_2$ was set in such a way that the absolute deviation is smaller than 1×10^{-8} in quadruple-precision calculations.

Phase Diagrams for One Electron in the Field of Two Coulomb Centers

Figure 3a shows the (R, Z_a) phase diagram of one electron in the field of two equally charged centers, $q = Z_a/Z_b = 1$. The phase diagram exhibits two phases: one where the electron is localized at $z = 0$, the $(\rho, 0)$ phase, and the other where the electron is

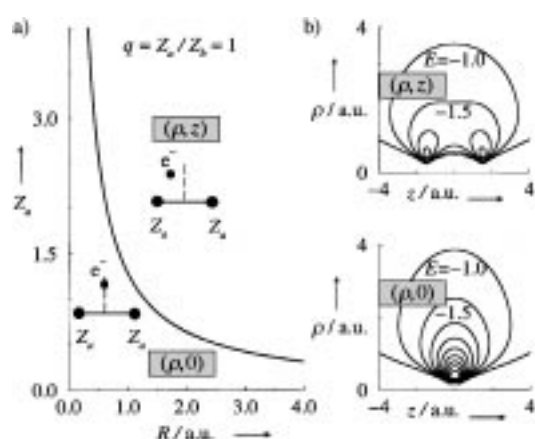


Figure 3. a) Phase diagram in the (R, Z_a) plane for one electron in the field of two equally charged centers $q = Z_a/Z_b = 1$ at the large-dimensional limit. b) The two different phases $(\rho, 0)$ and (ρ, z) are shown by plotting the corresponding potential energy. The phase $(\rho, 0)$ has a single minimum while the phase (ρ, z) is characterized by a double minimum.

localized on one or the other nucleus with $z \neq 0$, the (ρ, z) phase. The phase $(\rho, 0)$ is characterized by a single minimum in the potential energy, as shown in Figure 3b. The symmetry breaking, which splits the single minimum in the united atom limit into a double minimum in the separated atom limit, occurs along a critical line, $Z_a = (3\sqrt{3}/4)/R$. It is interesting to compare this continuous transition to the behavior in the phase space of a classical electron between two centers.^[25] One sees a separatrix bounding the region where the electron moves between the two centers. Outside of this region, the electron is primarily on either side. We have speculated^[25] that these two regions correspond to an electron moving “through bond” and “through space”, respectively, using the terminology favored in electron-transfer theory.

The $D \rightarrow \infty$ phase transition from an ionic to a covalent structure for one electron in the field of two centers of equal charge is the extreme limit of the familiar situation^[3] of the

changes in the charge distribution as one moves from separated centers to the united-atom limit.

The transition from one phase to the other is a continuous phase transition.^[26] By this, we mean that as we move across the phase plane the energies of the two isomers merge continuously as we cross the boundary. For the two phases shown, the (ρ, z) phase corresponds to ever smaller values of z until one reaches the boundary line on which it becomes identical to the $(\rho, 0)$ phase. The transition is continuous for any Z_a , as shown by an example in Figure 4. Such continuous changes in the electronic structure as, say, the internuclear distance is varied are familiar in many contexts and typically one does not think of them as corresponding to different isomers. Below, we shall identify first-order transitions where there is an abrupt and discontinuous change. For a first-order transition, which we will indicate by a dashed line, two different structures can coexist.

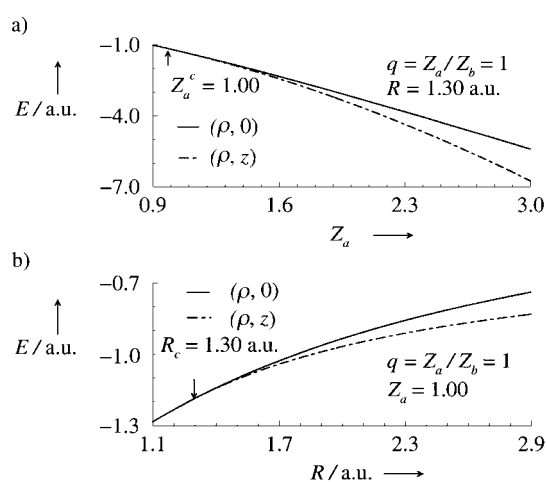


Figure 4. The energy-merging points for one electron in the field of two equally charged centers, $q = Z_a/Z_b = 1$, for a) $R = 1.30$ and $Z_b = 1.00$ and b) $Z_a = 1.00$ and $R_c = 1.30$.

We have checked that the transition is continuous in two directions $(\hat{e}_R, 0)$ and $(0, \hat{e}_Z)$ for each point on the boundary line. For example, in Figure 4 we show the energy merging points for $R = 1.30$ and for $Z_a = 1.00$ at fixed $q = 1$. As we already mentioned in the Introduction, for a second-order phase transition one expects the two energies to diverge quadratically as one moves away from the boundary line. This is very evident in Figure 4.

For unequal charges, $Z_a \neq Z_b$, on the two centers there is only one phase which corresponds to the electron localized on the higher charge center. This is to be contrasted with the familiar $D = 3$ case, Figure 2, which shows a more gradual shift of the charge localization. In the $D \rightarrow \infty$ limit, the ramp function shown in Figure 2 becomes an outright step function. The electron is either on the left or on the right side of the molecule, depending on the sign of ΔE .

The one-electron case has served to verify that the $D \rightarrow \infty$ limit does reproduce what we expect and we turn now to the far richer case of two electrons, a case where the Coulombic repulsion between the two electrons is explicitly present in the effective Hamiltonian of Equation (2).

Phase Diagrams for Two Electrons in the Field of Two Coulombic Centers

For two electrons in the field of two equally charged centers, $q = 1$, a study of the eigenvalues of Hessian matrix reveals the following:^[9] There are three different electronic phases $(\rho, 0; \rho, 0)$, $(\rho, z; \rho, -z)$, and $(\rho_1, 0; \rho_2, 0)$ as shown in Figure 5. The

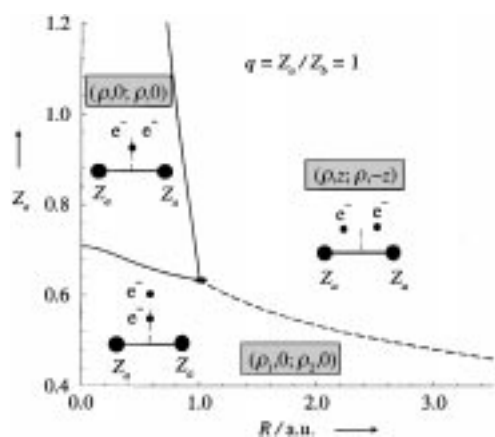


Figure 5. The phase diagram in the (R, Z_a) plane for two electrons in the field of two equally charged centers $q = Z_a/Z_b = 1$ at the large-dimensional limit. The continuous lines represent continuous phase transitions while the dashed line is a first-order phase transition line. The electron-dot representations of the three different stable phases are also shown.

phase $(\rho, 0; \rho, 0)$ corresponds to the symmetric electronic structure configuration where the two electrons are located in the symmetry plane $z = 0$ (z is defined by Equations (7) and (8)), at equal distances ρ from the two nuclei. The phase $(\rho, z; \rho, -z)$ has an nonsymmetric electronic configuration, the electrons are not in the symmetry plane $z = 0$ but occupy symmetric positions with respect to this plane. Another different nonsymmetric electronic configuration is $(\rho_1, 0; \rho_2, 0)$. This phase corresponds to both electrons in the symmetry plane $z = 0$ but with at different distances from the molecular axis. The electron-dot representation of the three different phases are also shown in Figure 5.

Inspection of Figure 5 helps in interpreting the nature of the three phases. Two of these, $(\rho, 0; \rho, 0)$, and $(\rho_1, 0; \rho_2, 0)$ are in the united-atom limit, $R \rightarrow 0$. That there are two structures in this limit is the simplest illustration of the importance of the Coulombic repulsion between the two electrons. When the charge on the nucleus is high, it overcomes the repulsion and the stable configuration is symmetric, $(\rho, 0; \rho, 0)$. But when the charge is lowered the repulsion dominates, and it is more favorable for the two electrons to occupy inequivalent locations. As the two centers move apart, the covalent structure $(\rho, z; \rho, -z)$ dominates. In this structure, the two electrons are symmetrically placed, such that $r_{a1} = r_{b2}$ and $r_{b1} = r_{a2}$.

If the stability lines of two different phases are coincident, then the phase transition is continuous. In such a case, one structure continuously deforms into the other as one approaches the boundary line. But, if the stability lines are not coincident, a coexistence phase appears, where two or more

structures correspond to local minima of the energy. A first-order phase transition line is therefore defined as the line where the global minimum is degenerate with two different phases having the same energy. This is when we say that two, or more, isomers are possible.

The results of examining the stability limits of the different phases, are also shown in Figure 5. The solid boundary lines separate the regions where the transition is continuous, and the first-order transitions are indicated as dashed boundary lines. Detailed numerical calculations show that there is a bicritical point at $(R, Z_a) = (1.00, 0.63)$. The bicritical point is the point where the first-order transition line splits into two critical lines.

For the case of unequal charges $q \neq 1$, such as HeH^+ -like systems, the electronic phase diagram is completely different from the case $q = 1$. Figure 6 shows that there are only two different phases: the covalent phase $(\rho_1, z_1; \rho_2, z_2)$ and the ionic phase $(\rho, z; \rho, z)$. The solid line represents a continuous phase transition while the dashed one represents a first-order phase transition. The special point where the first-order line meets with the continuous line has particular critical properties and is called tricritical point. This point was calculated as the point where the symmetric solution degenerates at $(R, Z_a) = (1.36, 1.30)$.

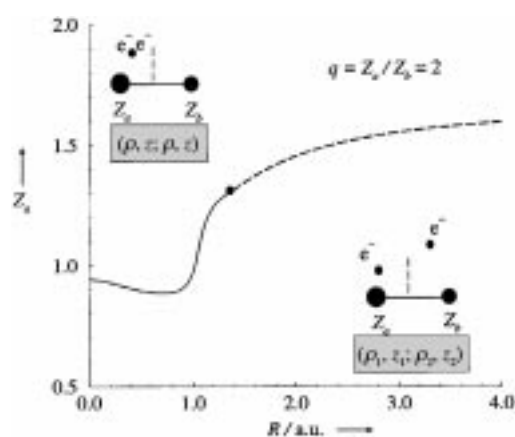


Figure 6. The phase diagram in the (R, Z_a) plane for two electrons in the field of two unequally charged centers, $q = Z_a/Z_b = 2$, at the large-dimensional limit. The continuous line represents a continuous phase transition while the dashed line is a first-order phase transition line. The phase diagram is characterized by a tricritical point. The electron-dot representations of the two different stable phases are also shown.

Figure 7 shows the merging on the energy line corresponding to the two different phases. This is characteristic of a continuous phase transition, whereas Figure 8 shows the crossings of the two energy lines as it should be in a first-order phase transition. The phase diagram for $q = 2$ is typical for all systems of $q \neq 1$. The electronic phase diagrams as the parameter q varies between 1.6 and 4 are shown in Figure 9. For systems with $q > 2$ a crossover phenomenon occurs; there is a value of R for which the system jumps from first-order phase transitions to continuous phase transitions.

There are a number of interesting features in the phase diagram for the case of two electrons. The most important one for us is the first-order phase transition between the ionic and

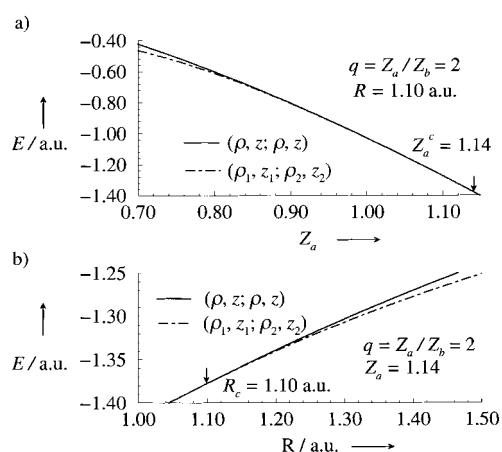


Figure 7. The energy-merging points for two electrons in the field of two unequally charged centers, $q = Z_a/Z_b = 2$, for a) $R_c = 1.10$ and $Z_c = 1.14$ and b) $Z_c = 1.14$ and $R_c = 1.10$.

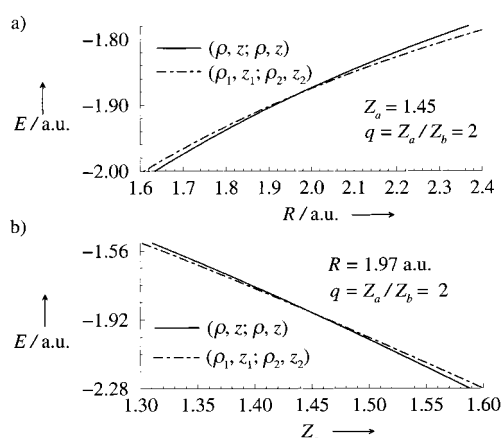


Figure 8. The energy-intersection points for two electrons in the field of two unequally charged centers, $q = Z_a/Z_b = 2$, for a) $Z_a = 1.45$ and $R_c = 1.97$ and b) $R = 1.97$ and $Z_c = 1.45$.

covalent phases, which is possible when the charges on the two centers are not the same. As can be seen from Figures 5–9, the transition is possible both when the internuclear distance R is varied for fixed site energies or when the energies are varied at a fixed distance.

Discussion

The motivation for this examination of the phase diagram of two-electron systems was to explore the interplay of three physical parameters, the difference in the energy of the two sites, the strength of the electronic coupling between the two sites, and the interelectronic Coulombic repulsion. For hydrogenlike atoms the site energy scales as Z^2 . The fractional difference in the energy of the two sites can therefore be measured by $q-1$, where q , as earlier defined, is the charge imbalance. The interelectronic repulsion is here taken at its full, unscreened value. We know that the binding energy of H^- is about 0.75 eV. The charging energy^[4, 21] of a hydrogen atom is therefore high and so the strong repulsion is realistic. The third

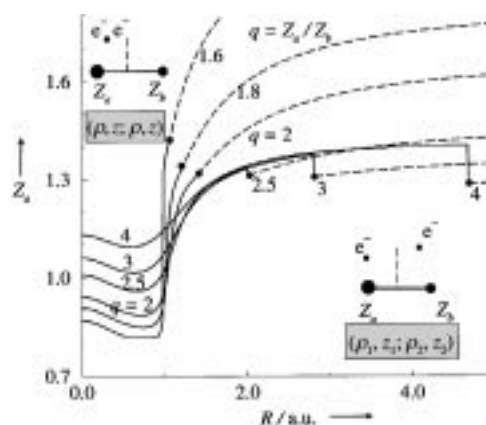


Figure 9. The phase diagram in the (R, Z_a) plane for two electrons for different values of q . The continuous line represents a continuous phase transition while the dashed line is a first-order phase transition line. The phase diagram is characterized by a tricritical point. The electron-dot representations of the two different stable phases are also shown.

parameter is here realized as the Coulombic attraction of electron 1 to nucleus b and of electron 2 to nucleus a . This surely scales with the distance between the two sites. So the phase diagram one ultimately would like to inspect is the one showing $q-1$ versus either R or a decreasing function of R . The two choices are dictated by different considerations. The parameter R is a variable subject to experimental control. A decreasing function of R is of more interest to theorists because the strength of the electronic coupling between the two sites increases as R decreases. The results are shown in Figures 10 and 11. In order to

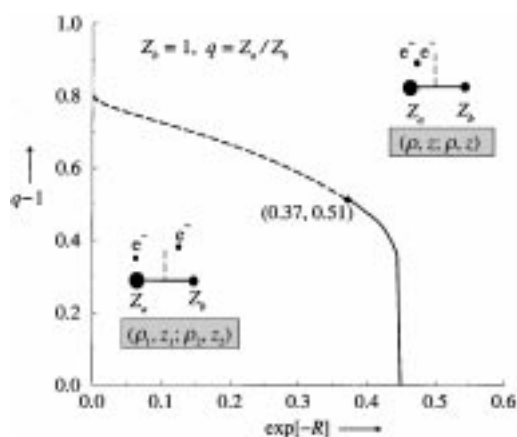


Figure 10. The phase diagram in the $(q-1, \exp[-R])$ plane for two electrons for fixed value of $Z_b = 1$. The continuous line represents a continuous phase transition while the dashed line is a first-order phase transition line.

relate the Figures to what is plotted in other contexts, one should first note that the “ordered” regime, which corresponds to the two charges being equal, $q = 1$, is at the bottom of the plot. Moving up the ordinate corresponds to increasing dissimilarity of the two sites; the abscissa points in the direction of weaker electronic coupling between them. As long as the two sites are identical or nearly so, the covalent phase prevails,

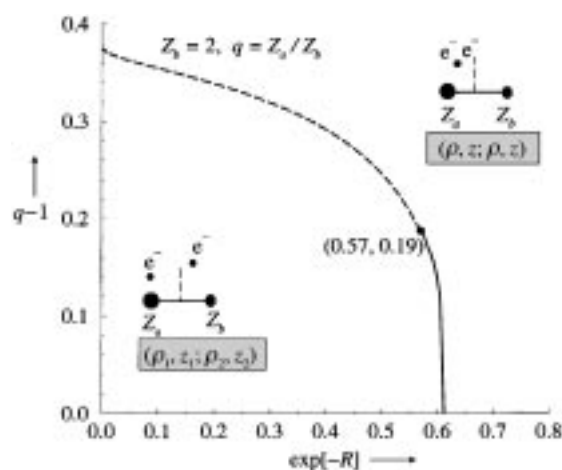


Figure 11. The phase diagram in the $(q - 1, \exp[-R])$ plane for two electrons for fixed value of $Z_b = 2$.

provided that the coupling strength is high. As the coupling strength is decreased there is a second-order (continuous) phase transition to an ionic state. This is what is also found for $D=3$. The one apparent difference is that for $D=3$ and $q=1$ the transition will be to an ionic state with one electron on each site. For higher values of q the covalent phase is invariably dominant. In the range $0.51 < q < 0.8$ and strong coupling, there is a first-order phase transition: As R decreases and the coupling increases, the ionic localized state changes discontinuously into a covalent phase. If the charges on the two centers are higher, Figure 11, the first-order phase transition occurs even for lower values of q .

Concluding Remarks

Scaling the dimension is, at first sight, a not very transparent operation. But, as the extensive literature shows,^[6] what it effectively does is to increase the mass of the electron such that, in the large- D limit, only the centrifugal part of the kinetic energy remains. The electrons then settle into what is known as a Lewis structure so that their configuration is easily seen. Using this approach, we have discussed both discontinuous and continuous changes in the arrangement of the electrons. We have mapped these changes for a diatomic molecule, not only as function of the internuclear distance but also in terms of the Coulombic energies of attraction to the two centers. We also paid special attention to the role of the electrostatic repulsion between the electrons.

The discontinuous changes, called first-order phase transitions, deserve a special comment. Along a boundary, shown as a dashed line in Figures 6 and 9–11, two distinct electronic states have the same energy. This is what is known in spectroscopy as a conical intersection and is usually taken to be not possible for a diatomic molecule; the proof is by the “noncrossing” rule. However, the conventional proof assumes that only one molecular parameter is varied and that a two-state approxima-

tion (or, equivalently, a perturbation theory approximation) is sufficient. There are refined proofs of the noncrossing rule (such as ref. [20]). Our study, with more analytical details being given in the Appendix, shows that such intersections are possible when more than one parameter can be varied.

Appendix

In spheroidal coordinates (λ, μ) , the general form of the Hamiltonian at the large-dimension limit for two-electron molecules with two charged centers Z_a and Z_b takes the form of Equation (9), where i labels the two electrons 1 and 2 and $q = Z_a/Z_b$ is fixed, R is the distance between the two charged centers, and r_{12} is the distance between the two electrons.

$$\mathcal{H} = \sum_{i=1}^2 \left(\frac{2R^2}{(\mu_i^2 - R^2)(R^2 - \lambda_i^2)} - \frac{2(\lambda_i + \mu_i + \lambda_i q - \mu_i q)Z_a}{(\lambda_i^2 - \mu_i^2)q} \right) + \frac{2R}{r_{12}} \quad (9)$$

Ground-state energy is the minimum of \mathcal{H} , Equation (10).

$$E_\infty(Z_a, R) = \min_{\lambda_1, \mu_1; \lambda_2, \mu_2} \mathcal{H} \quad (10)$$

This condition leads to four variational equations, Equations (11) and 12, with $i, j = 1, 2$ and $i \neq j$.

$$\frac{\partial \mathcal{H}}{\partial \lambda_i} = \frac{4\lambda_i R^2}{(\lambda_i^2 - R^2)^2 (\mu_i^2 - R^2)} + \frac{2[2\lambda_i \mu_i (1 - q) + \lambda_i^2 (1 + q) + \mu_i^2 (1 + q)]Z_a}{(\lambda_i^2 - \mu_i^2)^2 q} + \frac{2R(\mu_i \mu_j \lambda_j - \lambda_i R^2)}{(r_{12})^3} = 0 \quad (11)$$

$$\frac{\partial \mathcal{H}}{\partial \mu_i} = \frac{4\mu_i R^2}{(\mu_i^2 - R^2)^2 (\lambda_i^2 - R^2)} + \frac{2((\lambda_i^2 + \mu_i^2)(q - 1) - 2\lambda_i \mu_i (1 + q))Z_a}{(\lambda_i^2 - \mu_i^2)^2 q} + \frac{2R(\lambda_i \lambda_j \mu_j - \mu_i R^2)}{(r_{12})^3} = 0 \quad (12)$$

The stability condition: The minimum energy condition Equation (10) implies that for a given solution of Equations (11) and (12) all the eigenvalues of the 4×4 Hessian matrix must be positive. The Hessian matrix of \mathcal{H} is symmetrical and, as a function of the four variables $\lambda_1, \mu_1, \lambda_2,$ and μ_2 , there are 4×4 matrix elements of the form $\frac{\partial^2 \mathcal{H}}{\partial \lambda_i^2}, \frac{\partial^2 \mathcal{H}}{\partial \mu_i^2}, \frac{\partial^2 \mathcal{H}}{\partial \lambda_i \partial \mu_i}$, and $\frac{\partial^2 \mathcal{H}}{\partial \lambda_i \partial \mu_j}$. The explicit expressions for these matrix elements are given by Equations (13)–(22).

$$\frac{\partial^2 \mathcal{H}}{\partial \lambda_1^2} = \frac{4(3\lambda_1^2 R^2 + R^4)}{(\lambda_1^2 - R^2)^3 (\mu_1^2 + R^2)} + \frac{R(12(\lambda_2 \mu_1 \mu_2 - \lambda_1 R^2)^2 - 4R^2(-2\lambda_1 \lambda_2 \mu_1 \mu_2 + (\lambda_1^2 + \lambda_2^2 + \mu_1^2 + \mu_2^2)R^2 - 2R^4))}{2(r_{12})^5} + \frac{4(-3\lambda_1^2 \mu_1 (q-1) - \mu_1^3 (q-1) + \lambda_1^3 (1+q) + 3\lambda_1 \mu_1^2 (1+q)) Z_a}{(\lambda_1^2 - \mu_1^2)^3 q} \quad (13)$$

$$\frac{\partial^2 \mathcal{H}}{\partial \lambda_1 \partial \mu_1} = \frac{-8\lambda_1 \mu_1 R^2}{(\lambda_1^2 - R^2)^2 (\mu_1^2 - R^2)^2} + \frac{2R(-2\lambda_1^2 \lambda_2 \mu_2 R^2 + \lambda_2 \mu_2 R^2 (\lambda_2^2 - 2\mu_1^2 + \mu_2^2 - 2R^2) + \lambda_1 \mu_1 (\lambda_2^2 \mu_2^2 + 3R^4))}{(r_{12})^5} + \frac{4(-(\lambda_1^3 (q-1)) - 3\lambda_1 \mu_1^2 (q-1) + 3\lambda_1^2 \mu_1 (1+q) + \mu_1^3 (1+q)) Z_a}{(\lambda_1^2 - \mu_1^2)^3 q} \quad (14)$$

$$\frac{\partial^2 \mathcal{H}}{\partial \lambda_1 \partial \lambda_2} = \frac{2R(\mu_1 \mu_2 R^2 (\mu_1^2 + \mu_2^2 - 2\lambda_1^2 - 2\lambda_2^2 - 2R^2) + \lambda_1 \lambda_2 (\mu_1^2 \mu_2^2 + 3R^4))}{(r_{12})^5} \quad (15)$$

$$\frac{\partial^2 \mathcal{H}}{\partial \lambda_1 \partial \mu_2} = \frac{2R(\lambda_2 \mu_1 R^2 (\lambda_2^2 + \mu_1^2 - 2\lambda_1^2 - 2\mu_2^2 - 2R^2) + \lambda_1 \mu_2 (\lambda_2^2 \mu_1^2 + 3R^4))}{(r_{12})^5} \quad (16)$$

$$\frac{\partial^2 \mathcal{H}}{\partial \mu_1^2} = \frac{4(3\mu_1^2 R^2 + R^4)}{(\mu_1^2 - R^2)^3 (-\lambda_1^2 + R^2)} + \frac{R(12(\lambda_1 \lambda_2 \mu_2 - \mu_1 R^2)^2 - 4R^2(-2\lambda_1 \lambda_2 \mu_1 \mu_2 + (\lambda_1^2 + \lambda_2^2 + \mu_1^2 + \mu_2^2)R^2 - 2R^4))}{2(r_{12})^5} - \frac{4(-3\lambda_1^2 \mu_1 (q-1) - \mu_1^3 (q-1) + \lambda_1^3 (1+q) + 3\lambda_1 \mu_1^2 (1+q)) Z_a}{(\lambda_1^2 - \mu_1^2)^3 q} \quad (17)$$

$$\frac{\partial^2 \mathcal{H}}{\partial \mu_1 \partial \lambda_2} = \frac{2R(\lambda_2 \mu_1 (\lambda_1^2 \mu_2^2 + 3R^4) + \lambda_1 \mu_2 R^2 (\lambda_1^2 + \mu_2^2 - 2\lambda_2^2 - 2\mu_1^2 - 2R^2))}{(r_{12})^5} \quad (18)$$

$$\frac{\partial^2 \mathcal{H}}{\partial \mu_1 \partial \mu_2} = \frac{2R(\mu_1 \mu_2 (\lambda_1^2 \lambda_2^2 + 3R^4) + \lambda_1 \lambda_2 R^2 (\lambda_1^2 + \lambda_2^2 - 2(\mu_1^2 + \mu_2^2 + R^2)))}{(r_{12})^5} \quad (19)$$

$$\frac{\partial^2 \mathcal{H}}{\partial \lambda_2^2} = \frac{4(3\lambda_2^2 R^2 + R^4)}{(\lambda_2^2 - R^2)^3 (-\mu_2^2 + R^2)} + \frac{4R(3(\lambda_1 \mu_1 \mu_2 - \lambda_2 R^2)^2 - R^2 (r_{12})^2)}{2(r_{12})^5} - \frac{4(-3\lambda_2^2 \mu_2 (q-1) - \mu_2^3 (q-1) + \lambda_2^3 (1+q) + 3\lambda_2 \mu_2^2 (1+q)) Z_a}{(\lambda_2^2 - \mu_2^2)^3 q} \quad (20)$$

$$\frac{\partial^2 \mathcal{H}}{\partial \lambda_2 \partial \mu_2} = \frac{-8\lambda_2 \mu_2 R^2}{(\lambda_2^2 - R^2)^2 (\mu_2^2 - R^2)^2} + \frac{2R(\lambda_2 \mu_2 (\mu_1^2 \lambda_1^2 + 3R^4) + \lambda_1 \mu_1 R^2 (\lambda_1^2 + \mu_1^2 - 2(\lambda_2^2 - \mu_2^2 - R^2)))}{(r_{12})^5} + \frac{4((1-q)\lambda_2 (\lambda_2^2 + 3\mu_2^2) + (1+q)\mu_2 (\mu_2^2 + 3\lambda_2^2)) Z_a}{(\lambda_2^2 - \mu_2^2)^3 q} \quad (21)$$

$$\frac{\partial^2 \mathcal{H}}{\partial \mu_2^2} = \frac{4(3\mu_2^2 R^2 + R^4)}{(\mu_2^2 - R^2)^3 (-\lambda_2^2 + R^2)} + \frac{4R(3(\lambda_1 \lambda_2 \mu_1 - \mu_2 R^2)^2 - R^2 (r_{12})^2)}{2(r_{12})^5} - \frac{4((1-q)\mu_2 (\mu_2^2 + 3\lambda_2^2) + (1+q)\lambda_2 (\lambda_2^2 + 3\mu_2^2)) Z_a}{(\lambda_2^2 - \mu_2^2)^3 q} \quad (22)$$

Symmetry-breaking configurations can be determined by studying the stability of the different solutions of the variational equations, Equations (11) and (12), as a function of Z_a , q , and R . We actually used Equations (9)–(22) to describe the stability of the nonsymmetrical electronic configurations. For the symmetrical structures $\lambda_2 = \lambda_1 = \lambda$ and $\mu_2 = \mu_1 = \mu$, which are equivalent to $\rho_1 = \rho_2 = \rho$ and $z_1 = z_2 = z$, the Hessian matrix elements take a much simpler form. Extensive analytical and numerical calculations show that there are only three different solutions corresponding to a global minimum for $q = 1$ and only two solutions corresponding to a global minimum for $q > 1$ in the region $R \geq 0$ and $q \geq 1$.

For the case $q = 1$, the variational equations take a simpler form which allows for some analytical results.^[9] One possible solution of Equations (11) and (12) is the symmetric solution with $\lambda_1 = \lambda_2 = \lambda$ and $\mu_1 = \mu_2 = 0$. This solution corresponds to the symmetric electronic structure configuration where the two electrons are located in the symmetry plane $z = 0$ with equal distances from the two nuclei. The symmetric solution of Equations (11), which relates λ to R and Z_a is given by Equation (23).

$$Z_a(R, \lambda) = \frac{[(\lambda^2 - R^2)^{1/2} + 2^{5/2}] \lambda^3}{2(\lambda^2 - R^2)^2} \quad (23)$$

This solution is a minimum in the region where all the eigenvalues of the Hessian matrix are positive. In this case, the two smallest eigenvalues of the Hessian matrix are given by Equations (24) and (25).

$$\Lambda_1^{(\text{sym})} = \frac{4(R^2 + 3\lambda^2)}{(\lambda^2 - R^2)^3} - \frac{8Z_a}{\lambda^3} - \frac{1}{2^{1/2}(\lambda^2 - R^2)^{3/2}} \quad (24)$$

$$\Lambda_2^{(\text{sym})} = \frac{4}{R^2(\lambda^2 - R^2)} - \frac{8Z_a}{\lambda^3} - \frac{\lambda^2 + R^2}{2^{1/2} R^2 (\lambda^2 - R^2)^{3/2}} \quad (25)$$

The stability limits are given by the condition $\Lambda_i^{(\text{sym})} = 0$ and Equation (23). These Equations give two cubic polynomials in which their roots are the stability limit lines of the symmetric solution. The point at which both eigenvalues are equal to zero gives the bicritical point ($R = 1$, $Z_a = 0.63$).

The symmetry-breaking solution of the variational equations can be obtained by defining $\lambda_1 = \lambda$, $\lambda_2 = \alpha\lambda$, and $\mu_1 = \mu_2 = 0$. This solution corresponds to both electrons in the symmetry plane $z = 0$ but at different distances from the molecular axis. Another different, nonsymmetric electronic configuration is given by the conditions $\lambda_1 = \lambda_2 = \lambda$ and $\mu_1 = \mu = -\mu_2$. This solution

corresponds to the electrons not being in the symmetry plane $z=0$ but occupying symmetric positions with respect to this plane. These three different solutions for the case $q=1$ are shown in Figure 5.

S.K. would like to acknowledge the financial support of ONR, NSF and the Forchheimer Foundation.

- [1] W. Fuss, W. E. Schmid, S. A. Trushin, *J. Chem. Phys.* **2000**, *112*, 8347.
- [2] G. C. Schatz, M. A. Ratner, *Quantum Mechanics in Chemistry*, Prentice-Hall, New York, NY, **1993**.
- [3] J. C. Slater, *Quantum Theory of Molecules and Solids*, McGraw-Hill, New York, NY, **1963**.
- [4] F. Remacle, R. D. Levine, *Proc. Natl. Acad. Sci. USA* **2000**, *97*, 553.
- [5] F. Remacle, C. P. Collier, J. R. Heath, R. D. Levine, *Chem. Phys. Lett.* **1998**, *291*, 453.
- [6] D. R. Herschbach, J. Avery, O. Gosinski, *Dimensional Scaling in Chemical Physics*, Kluwer, Dordrecht, **1993**.
- [7] D. R. Herschbach, *J. Chem. Phys.* **1986**, *84*, 838.
- [8] S. Sachdev, *Quantum Phase Transitions*, Cambridge University Press, New York, NY, **1999**.
- [9] P. Serra, S. Kais, *Chem. Phys. Lett.* **1996**, *260*, 302.
- [10] S. Kais, P. Serra, *Int. Rev. Phys. Chem.* **2000**, *19*, 97.
- [11] D. R. Yarkony, *Rev. Mod. Phys.* **1996**, *68*, 985–1013.
- [12] M. Desouter-Lecomte, D. Dehareng, B. Leyh-Nihant, M. Th. Praet, A. J. Lorquet, J. C. Lorquet, *J. Phys. Chem.* **1985**, *89*, 214–222.
- [13] H. C. Longuet-Higgins, *Proc. R. Soc. London A* **1975**, *344*, 147–156.
- [14] T. J. Lee, D. J. Fox, H. F. Schaefer, R. M. Pitzer, *J. Chem. Phys.* **1984**, *81*, 356.
- [15] E. Teller, *Isr. J. Chem.* **1969**, *7*, 227–235.
- [16] C. Zener, *Proc. R. Soc. London A* **1932**, *137*, 696–702.
- [17] J. von Neumann, E. P. Wigner, *Phys. Z.* **1929**, *30*, 467.
- [18] L. D. Landau, E. M. Lifshitz, *Quantum Mechanics*, Butterworth-Heinemann, Oxford, **1997**.
- [19] G. J. Hatton, W. L. Lichten, N. Ostrove, *J. Chem. Phys.* **1977**, *67*, 2169–2177.
- [20] C. A. Mead, *J. Chem. Phys.* **1979**, *70*, 2276–2283.
- [21] F. Remacle, R. D. Levine, *J. Am. Chem. Soc.* **2000**, *122*, 4084.
- [22] M. L. Cabrera, A. L. Tan, J. G. Loeser, *J. Phys. Chem.* **1993**, *97*, 2467; A. L. Tan, Ph.D. thesis, Harvard University (USA), **1994**.
- [23] G. Hunter, H. O. Pritchard, *J. Chem. Phys.* **1967**, *46*, 2146.
- [24] W. H. Press, S. A. Teukolsky, W. T. Vetterling, B. P. Flannery, *Numerical Recipes in Fortran, The Art of Scientific Computing*, Cambridge University Press, New York, NY, **1992**.
- [25] F. Remacle, R. D. Levine, *J. Chem. Phys.* **2000**, *113*, 4515.
- [26] P. Serra, S. Kais, *Phys. Rev. Lett.* **1996**, *77*, 466.
- [27] M. Klessinger, J. Michl, *Excited States and Photochemistry of Organic Molecules*, VCH, New York, NY, **1995**.

Received: December 1, 2000 [F158]